# Singularity analysis: A poweful technique for scatterometer wind data processing

*M. Portabella (ICM-CSIC)*
*W. Lin (ICM-CSIC)*
*A. Stoffelen (KNMI)*
*A. Turiel (ICM-CSIC)*
*G. King (ICM-CSIC)*
*A. Verhoef (KNMI)*

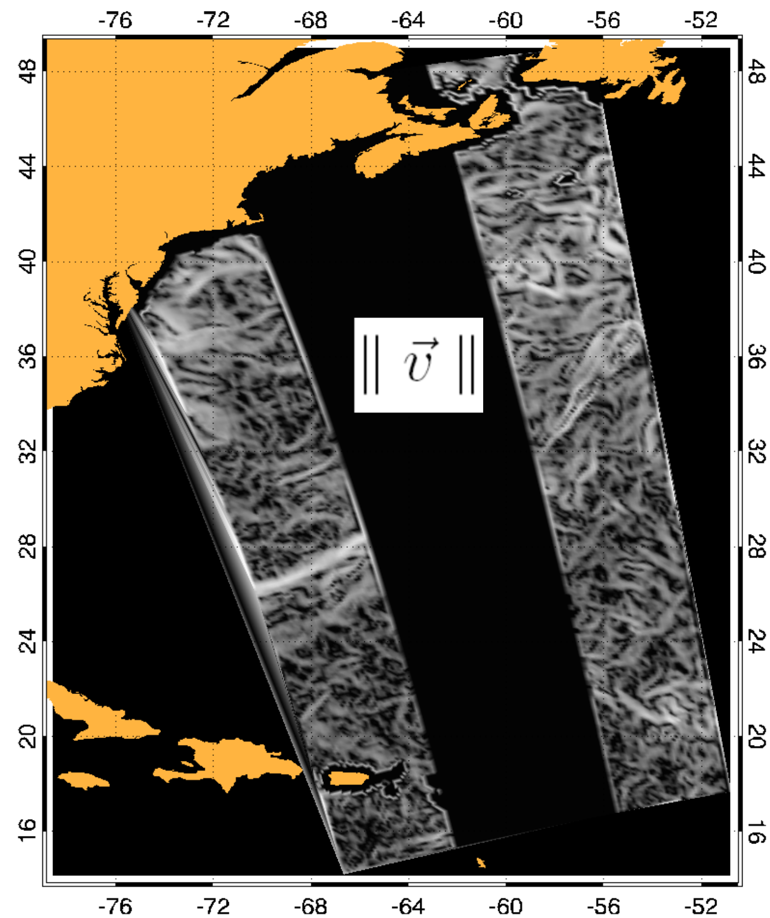

# Singularity analysis

SA is a technique to extract relevant structures from maps of scalar variables, in connection with turbulence theory.

The singularity exponents h(x) at each point x are calculated according the following formula:

$$\boxed{T_\Psi |\nabla\theta|(\vec{x}, r) \equiv \int d\vec{x}' \, |\nabla\theta|(\vec{x}')\Psi\left(\frac{\vec{x}-\vec{x}'}{r}\right) = \alpha_\Psi(\vec{x}) r^{h(\vec{x})} + o\left(r^{h(\vec{x})}\right)}$$

## Singularity analysis for dynamic assessment of flows

- Singularity exponents are dimensionless, spatially coherent and unaffected by changes in local amplitude.
- They are hence very useful to detect structures, even subtle.
- Singularity analysis is specially effective when the system under analysis is of a special, scale-invariant type (multifractal, MF).
- The archetypes of MF systems are turbulent flows. Singularity analysis is very effective in the ocean and the atmosphere.

## Earth Simulator

# $\sigma_h = 0{,}15$

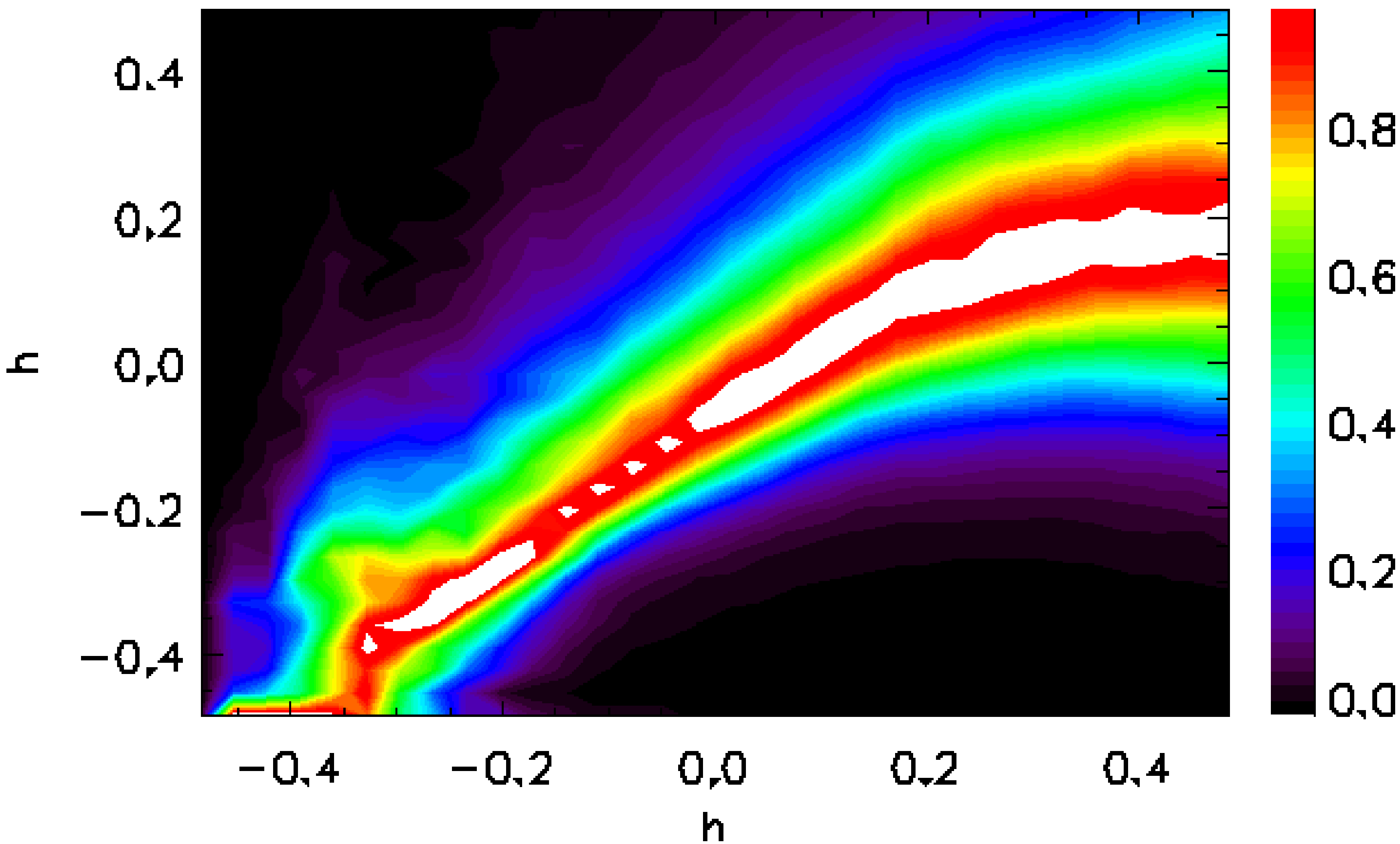

# Singularity exponents track streamlines

A comparison with high-resolution altimetry reveals that singularity lines from MW SST are very close to streamlines

A. Turiel et al., Ocean Sciences (2009)

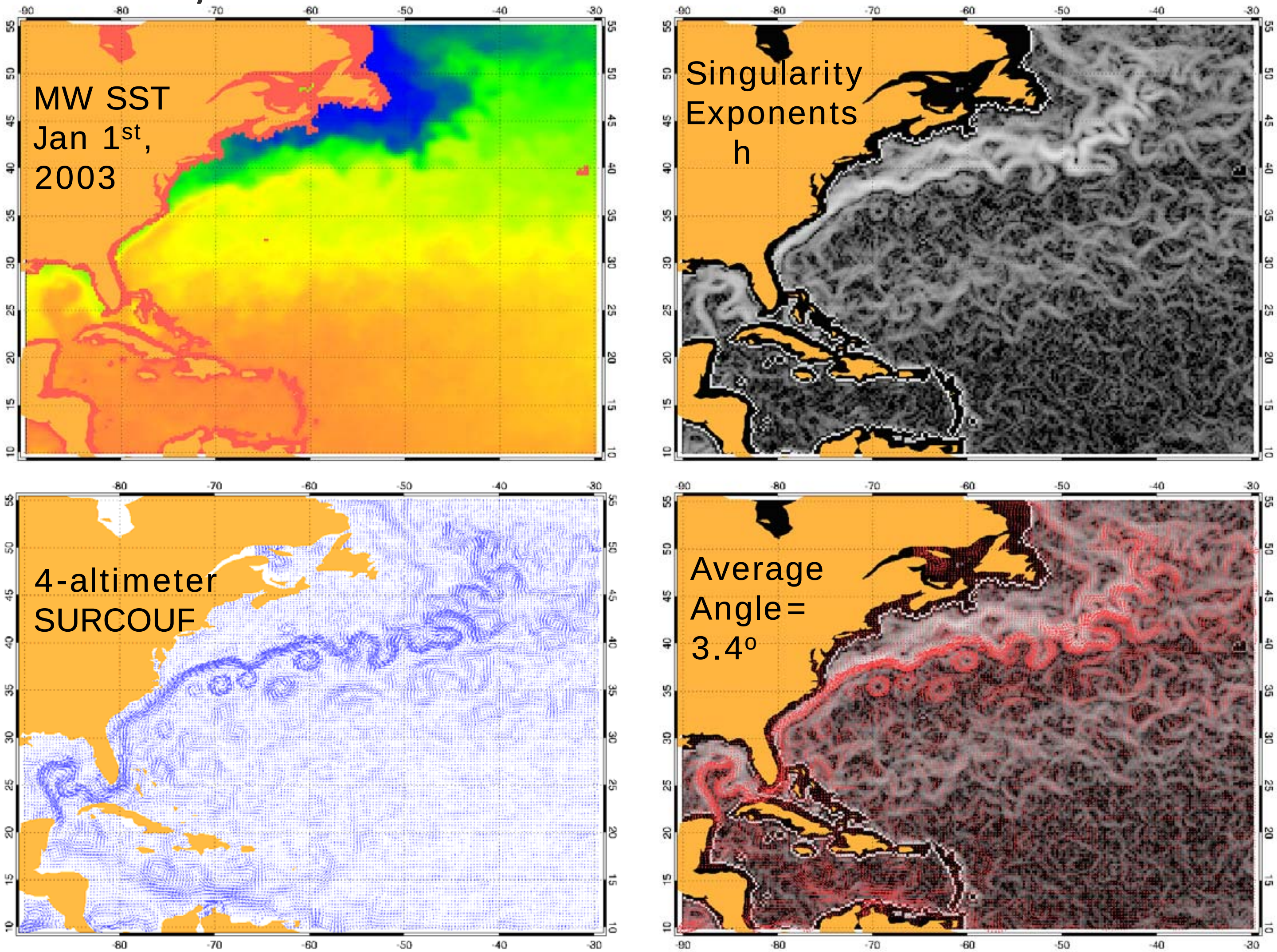

# Scalar sinergy

The action of advection on ocean scalars (passive, active and reactive) makes the singularity structure of all ocean scalars to correspond

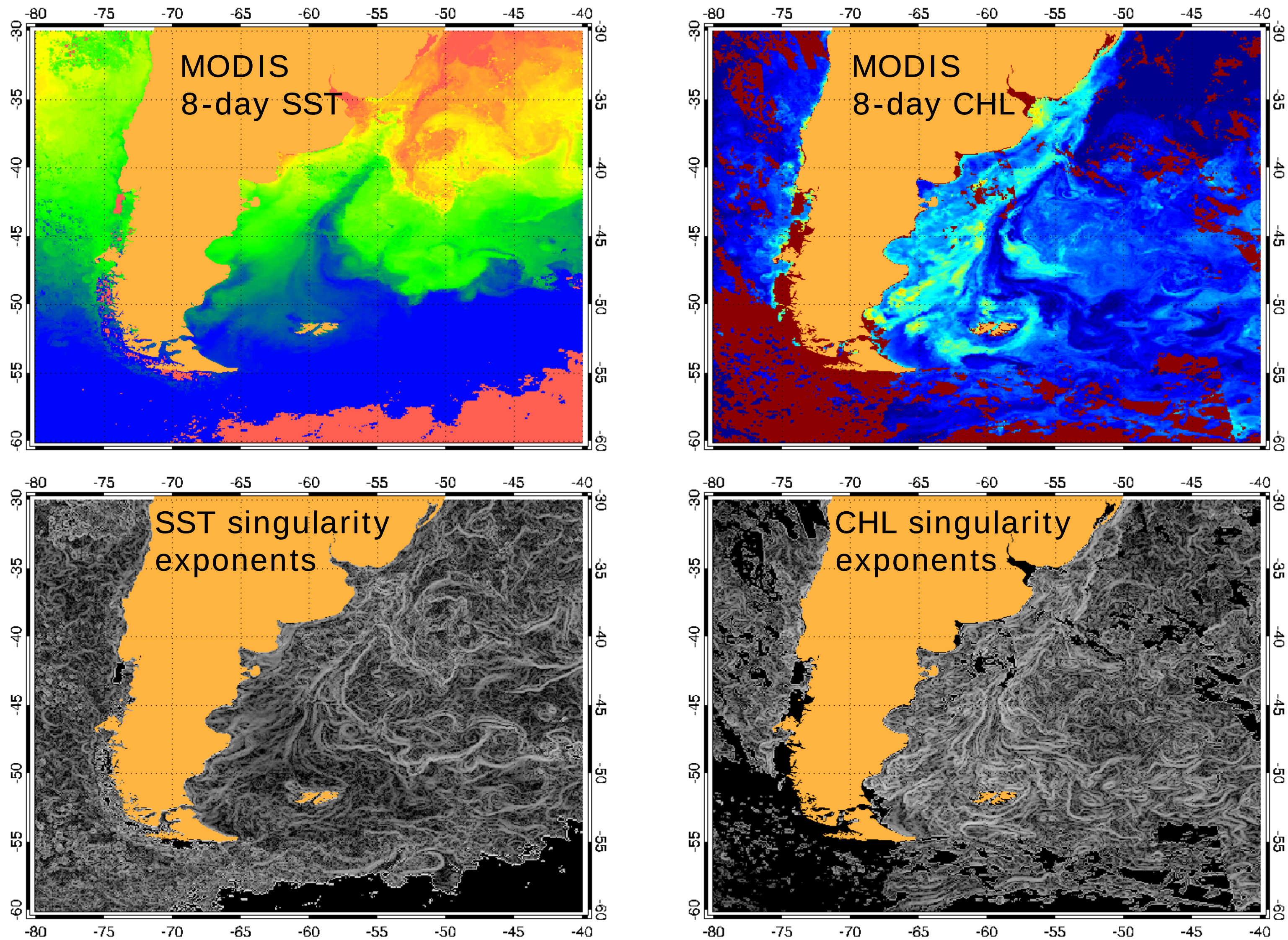

L4 products are visually better. We can recognise in them some structures not evident nor in SST maps either in L3 SMOS maps.

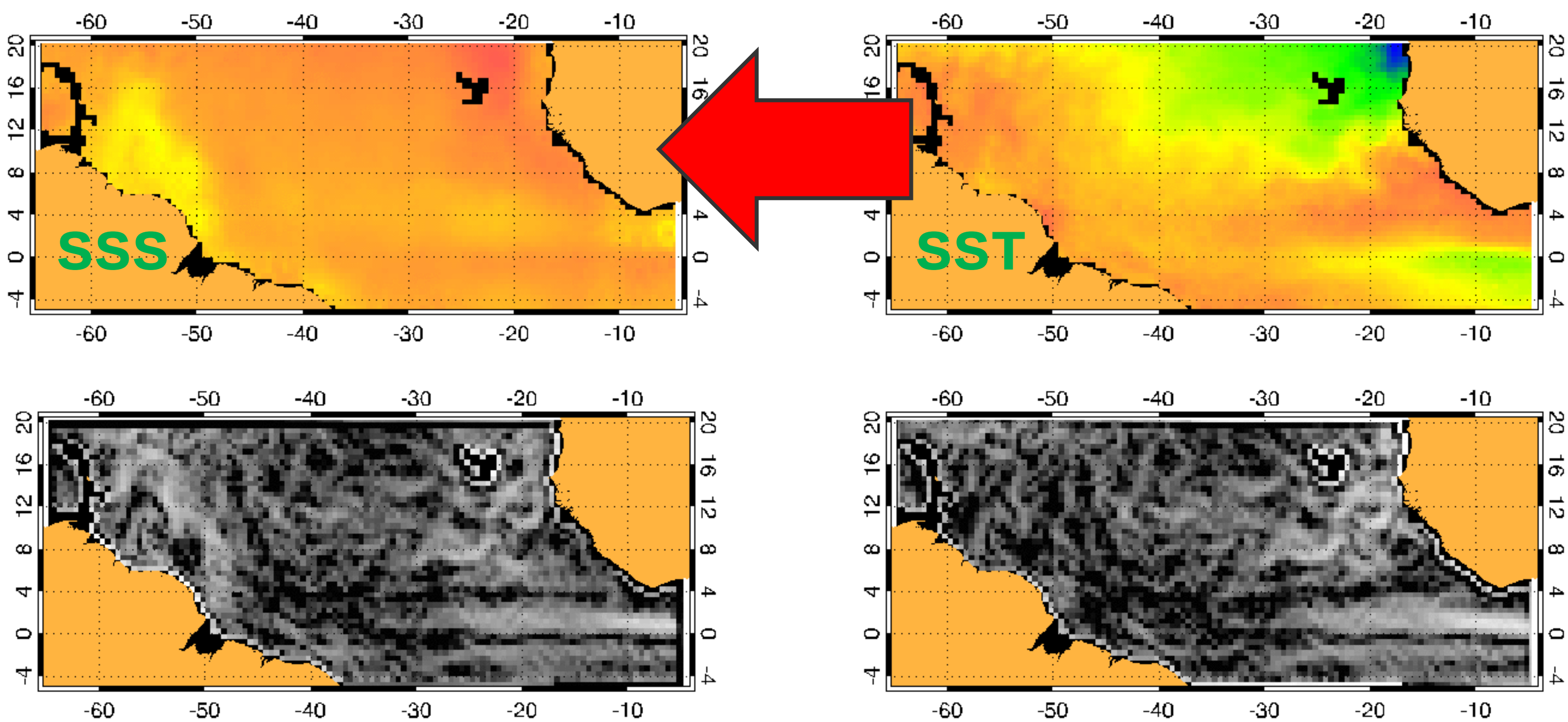


They lead to a considerable increase in quality (0.3)

# SA allows to detect mismatches in component separation

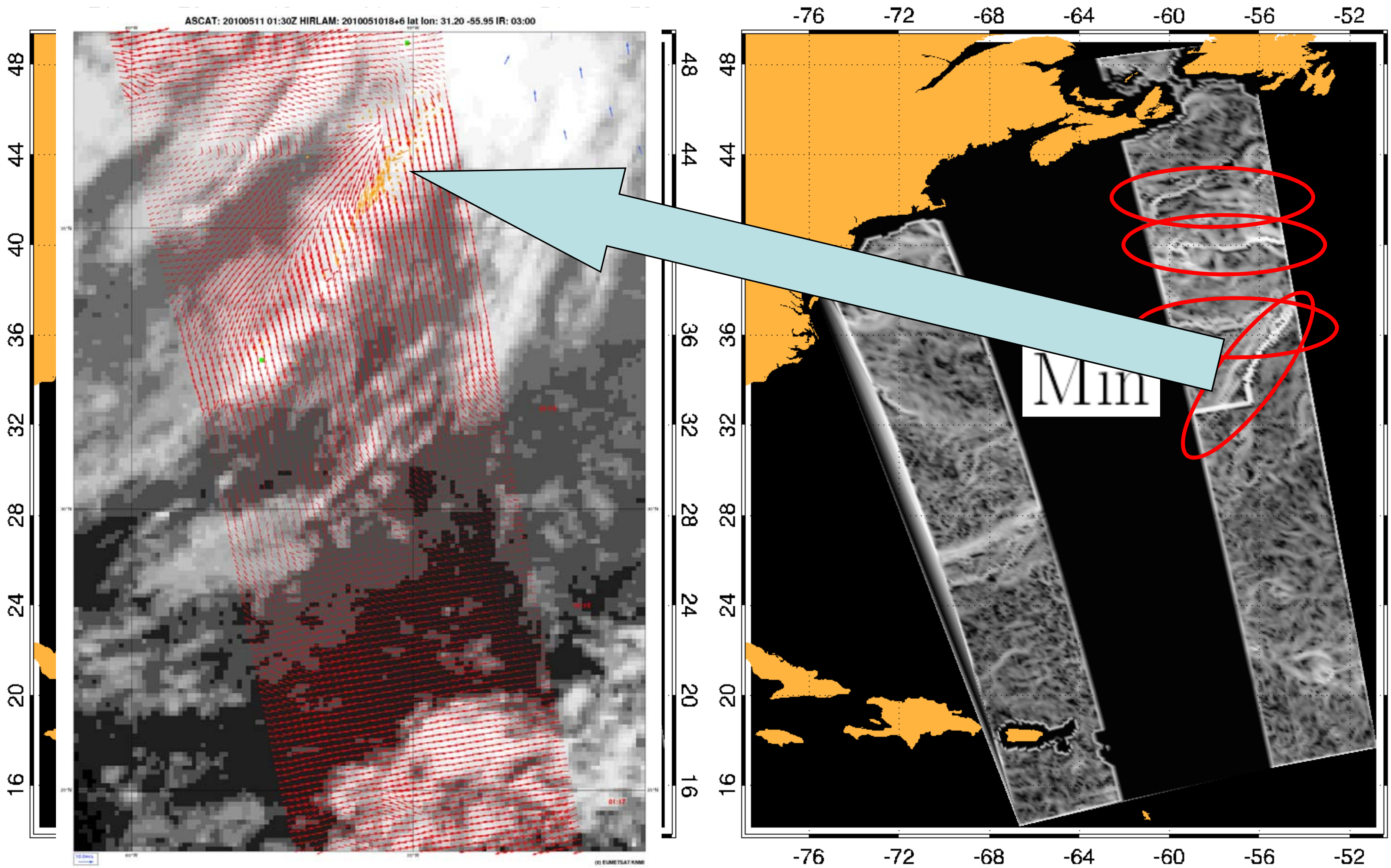

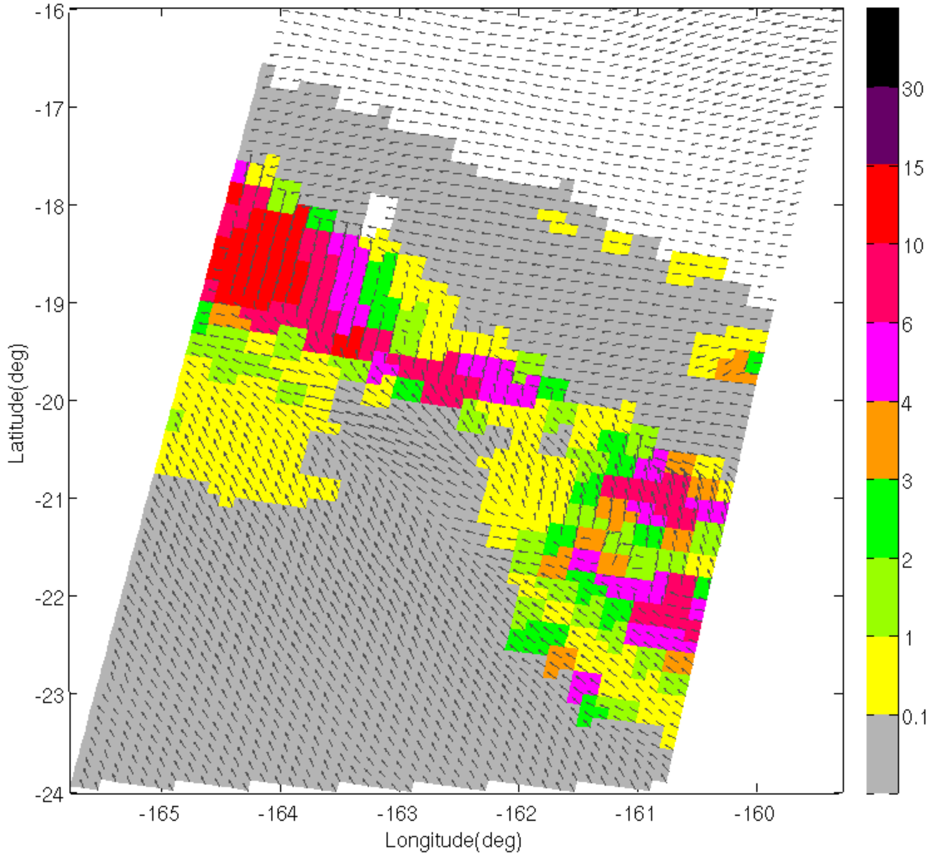


ASCAT-derived wind field collocated with TMI RR data at 20:30 UTC on 24 September 2008

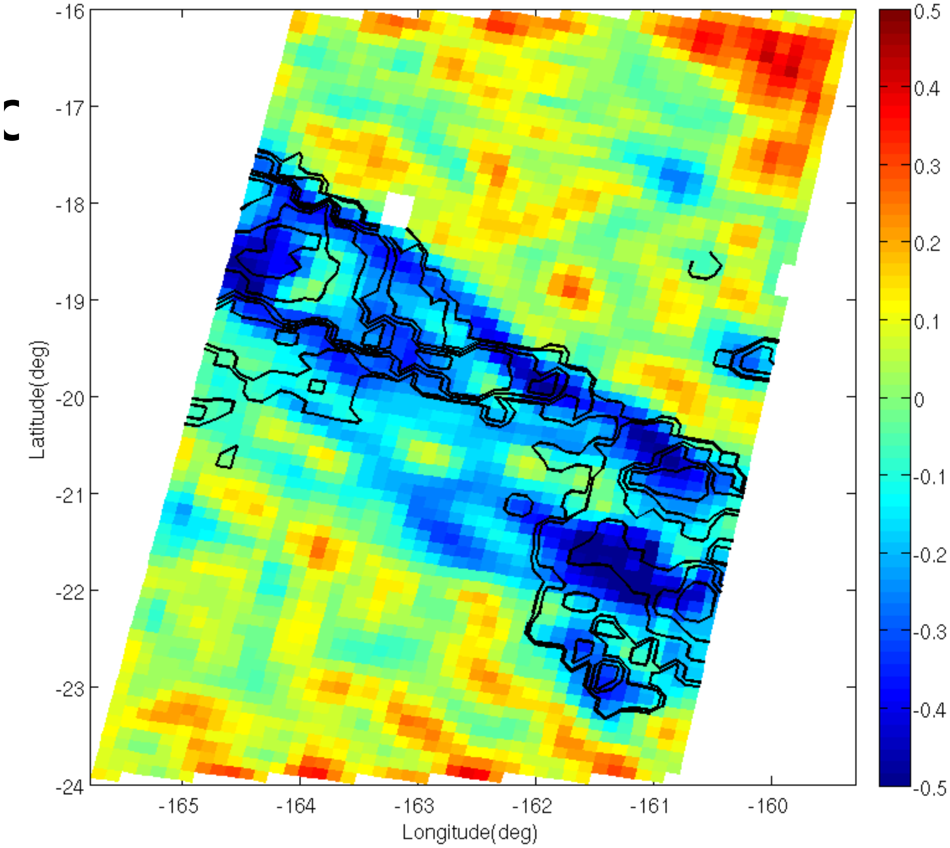


Singularity map of the ASCAT-retrieved wind field. TMI RR data shown as contour lines

- **Good correspondance between TMI RR and negative SE values**

***Portabella et al., TGRS, 2012***
***Lin et al., GRSL, 2014***

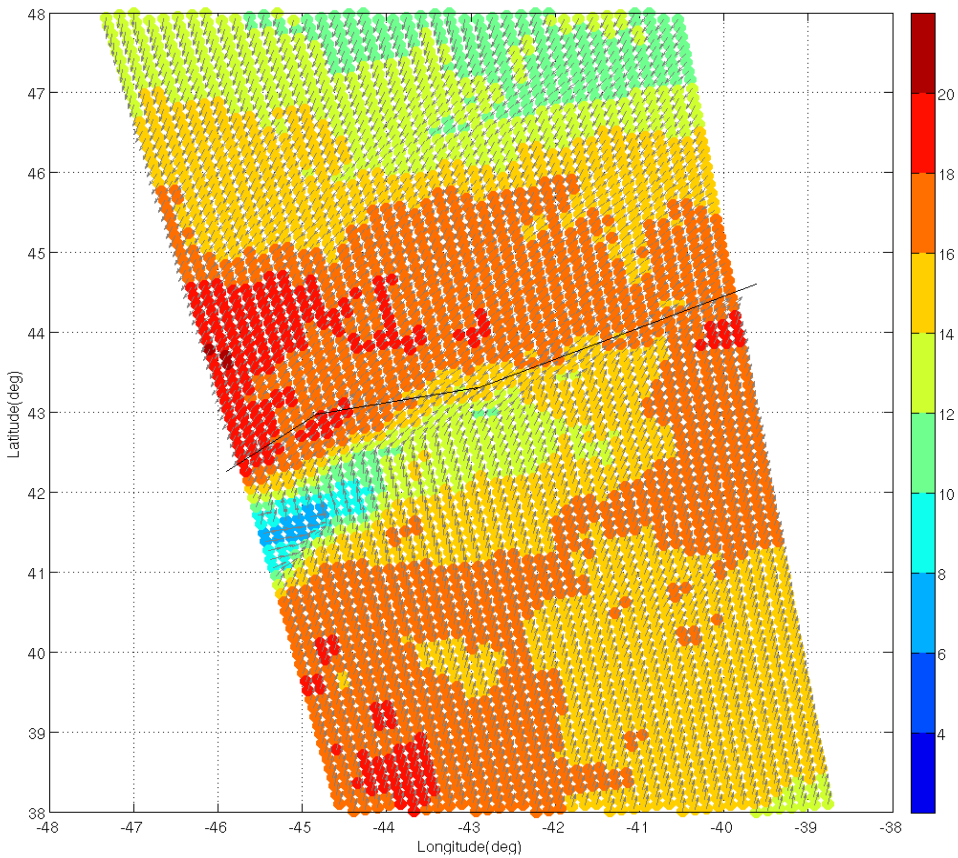


ASCAT-derived wind field at 00:15
December 15 2011

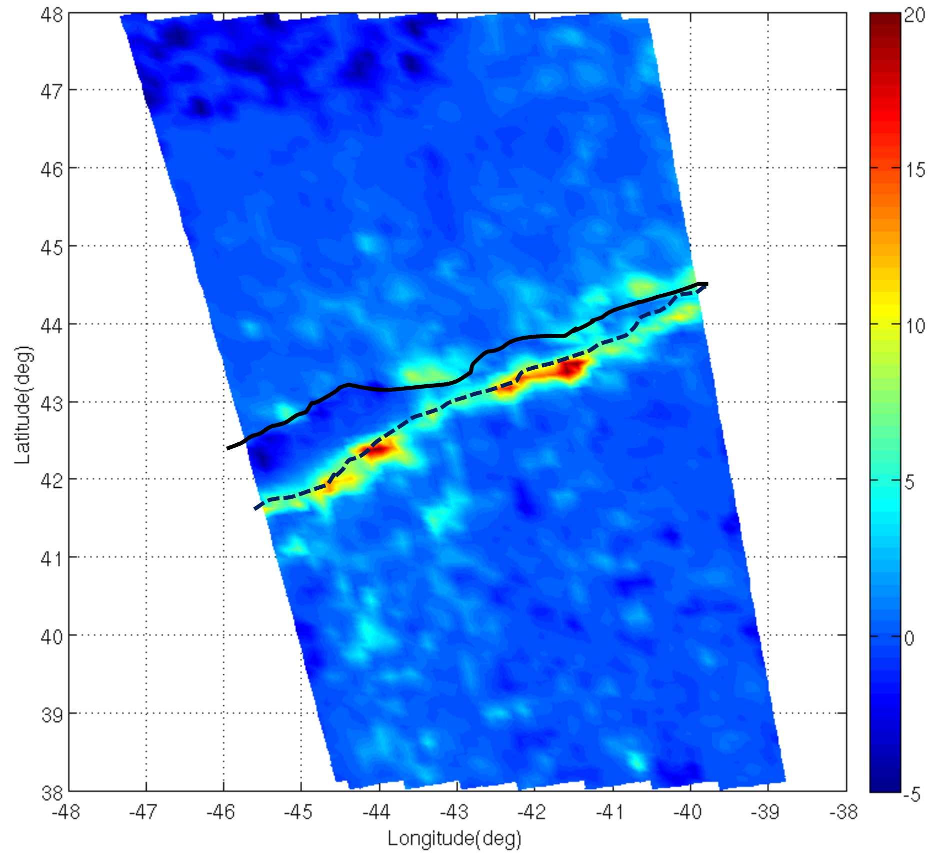


ASCAT-derived MLE distribution

- **Solid line shows ASCAT-derived wind front (convergence)**
- **Dotted line shows front as detected by MLE analysis**

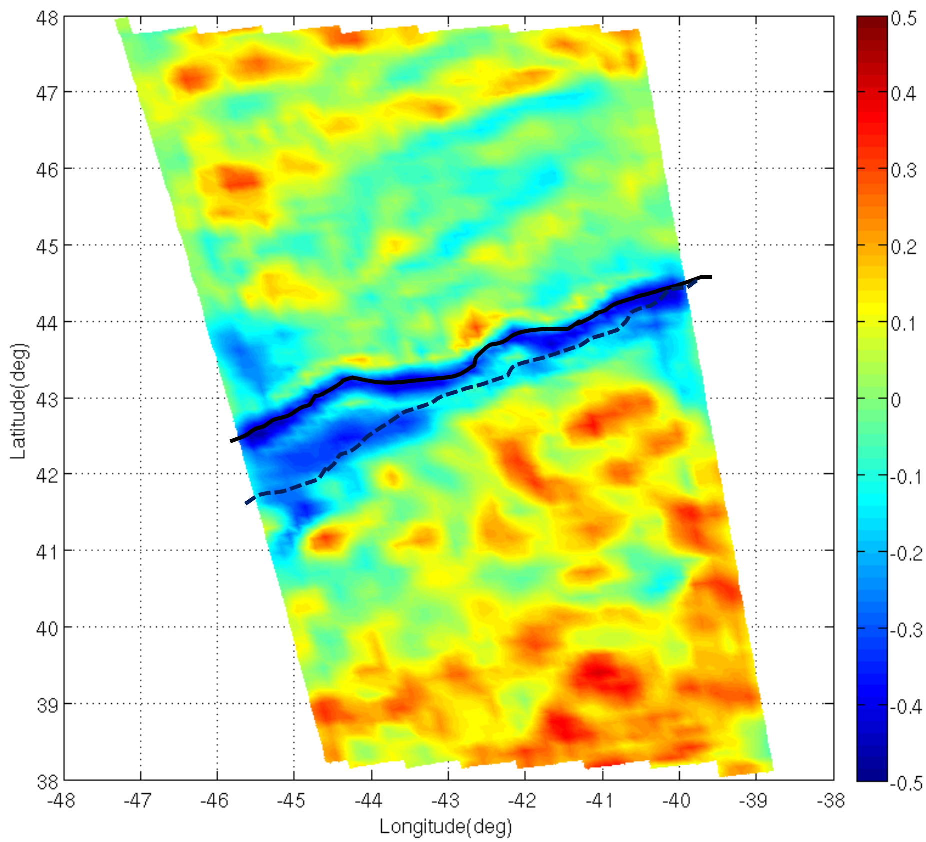


Singularity map from ASCAT U and V

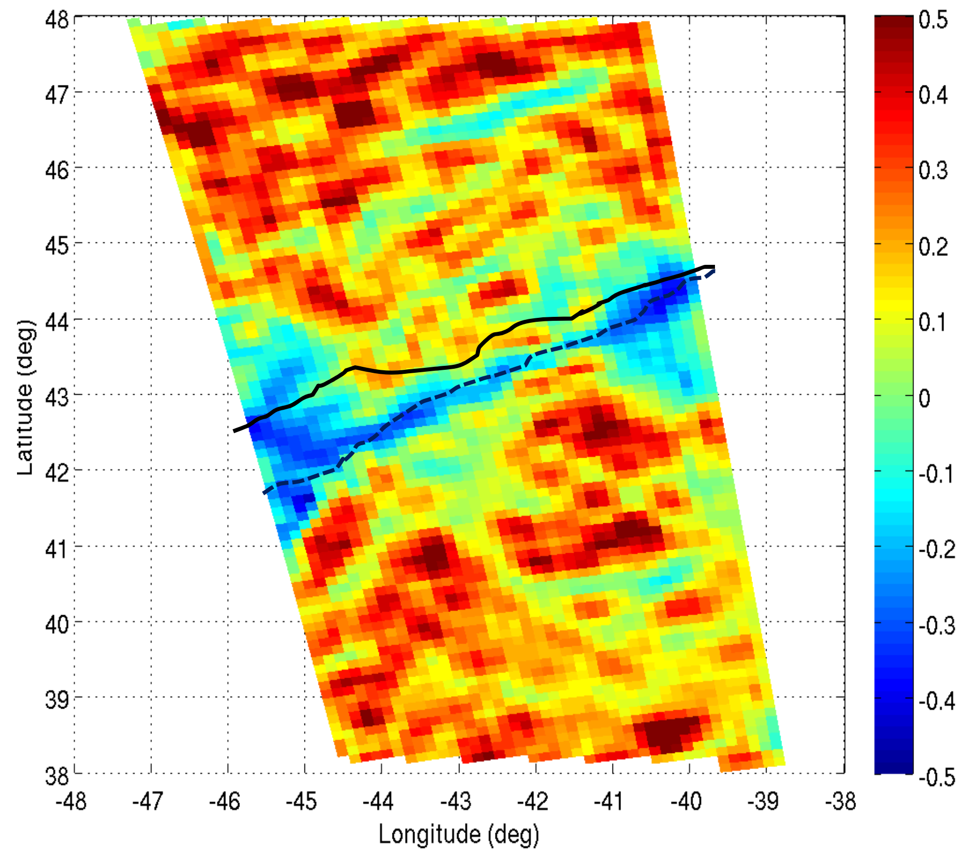


Singularity map from modified ASCAT direction

<u>Modified direction</u>:

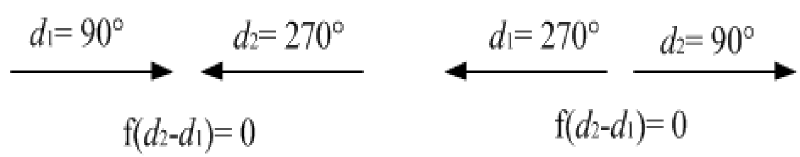


- **AR errors propagate into singularity analysis computation**
- **Modified direction insensitive to AR errors**

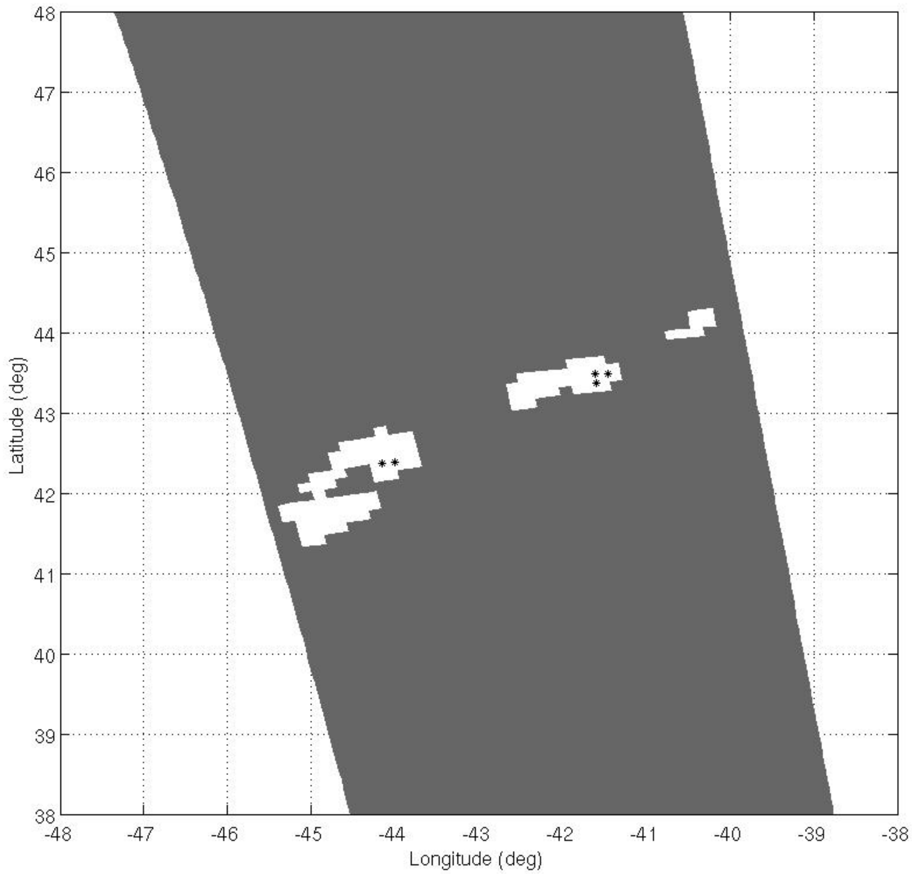


WVCs with SE<-0.4
MLE-based QC denoted by the asterisks

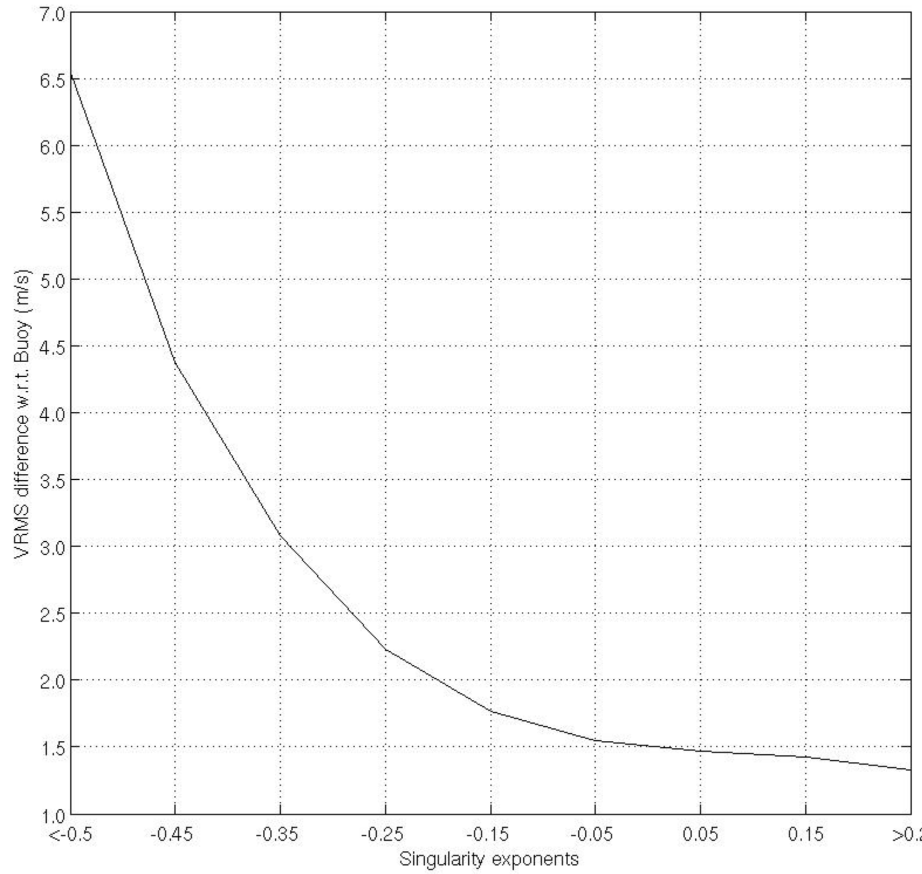


Mean Vector RMS (VRMS) difference between ASCAT selected solutions and buoy winds

- **Stronger filtering of SE-based QC along front w.r.t. MLE-based QC**
- **Clear relation between SE value and ASCAT wind quality**

# C-band Quality control

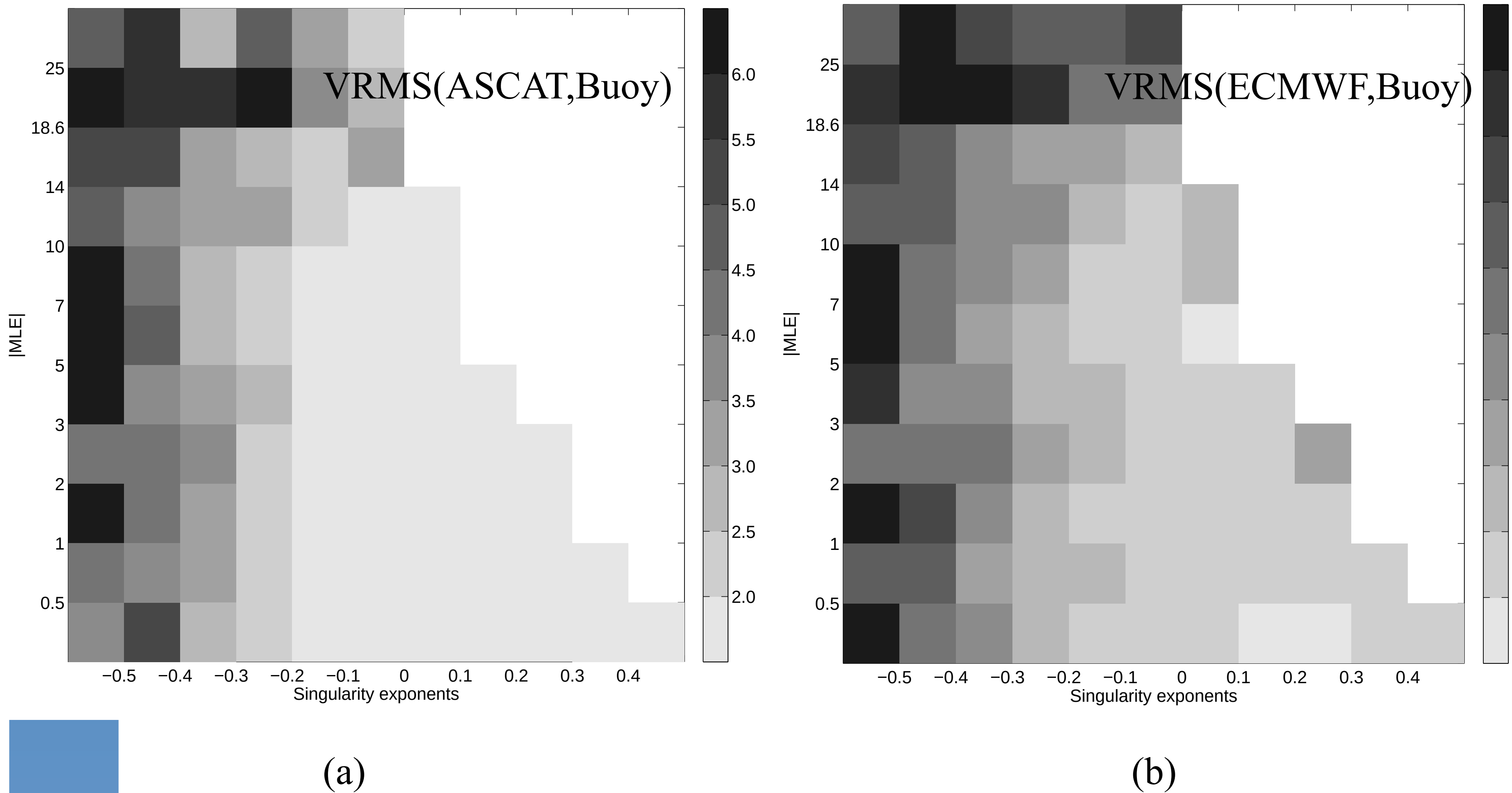


Fig. 1 The VRMS difference between buoy and (a) ASCAT winds; (b) ECMWF winds, as a function SE and MLE.

- The correspondence of buoy, ASCAT and ECMWF winds reduces as SE decreases and MLE increases
- SE and MLE parameters are complementary in terms of quality classification

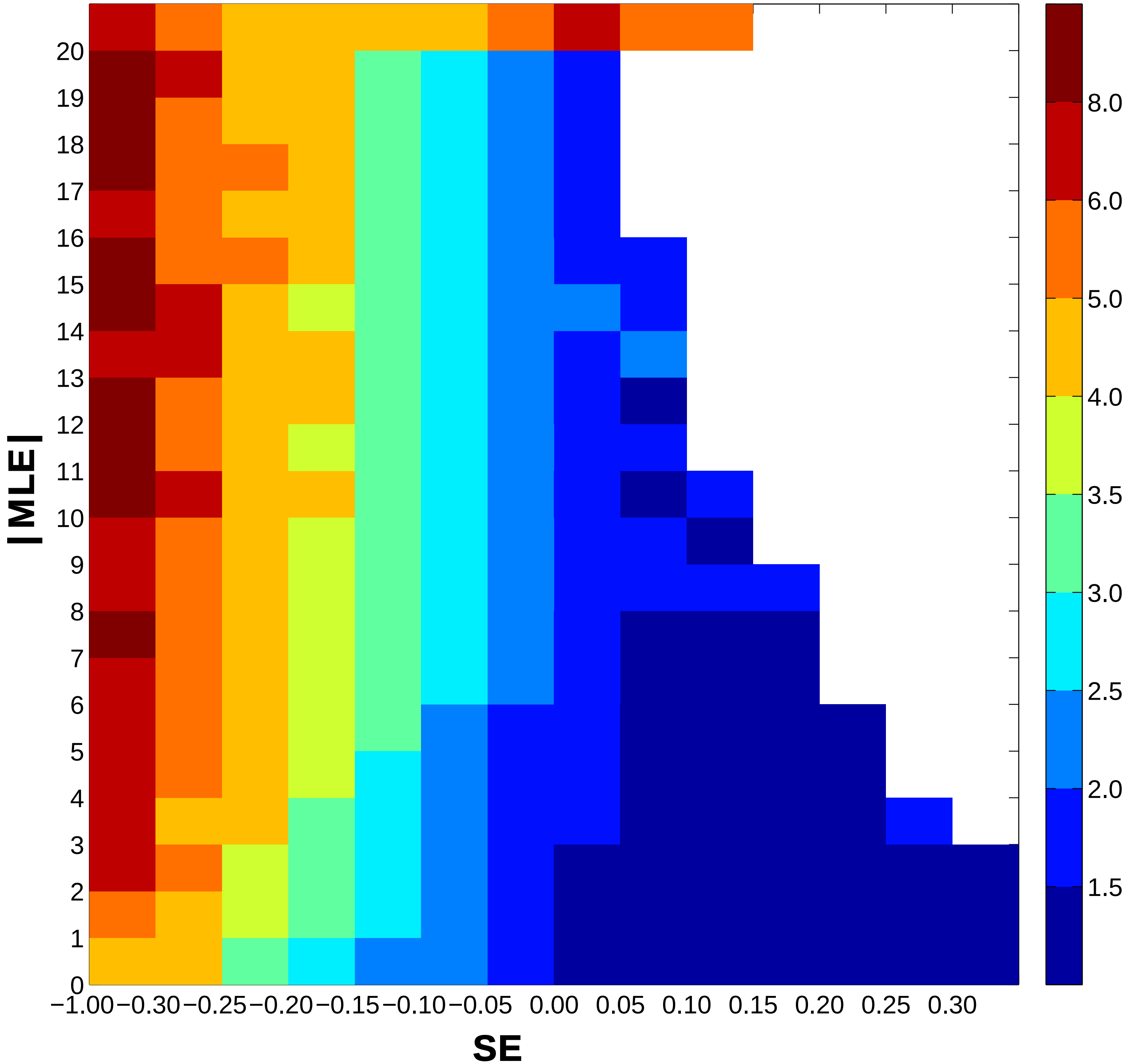


VRMS difference between RSCAT and ASCAT as a function of SE (x-axis) and MLE (y-axis)

# C-band Quality control

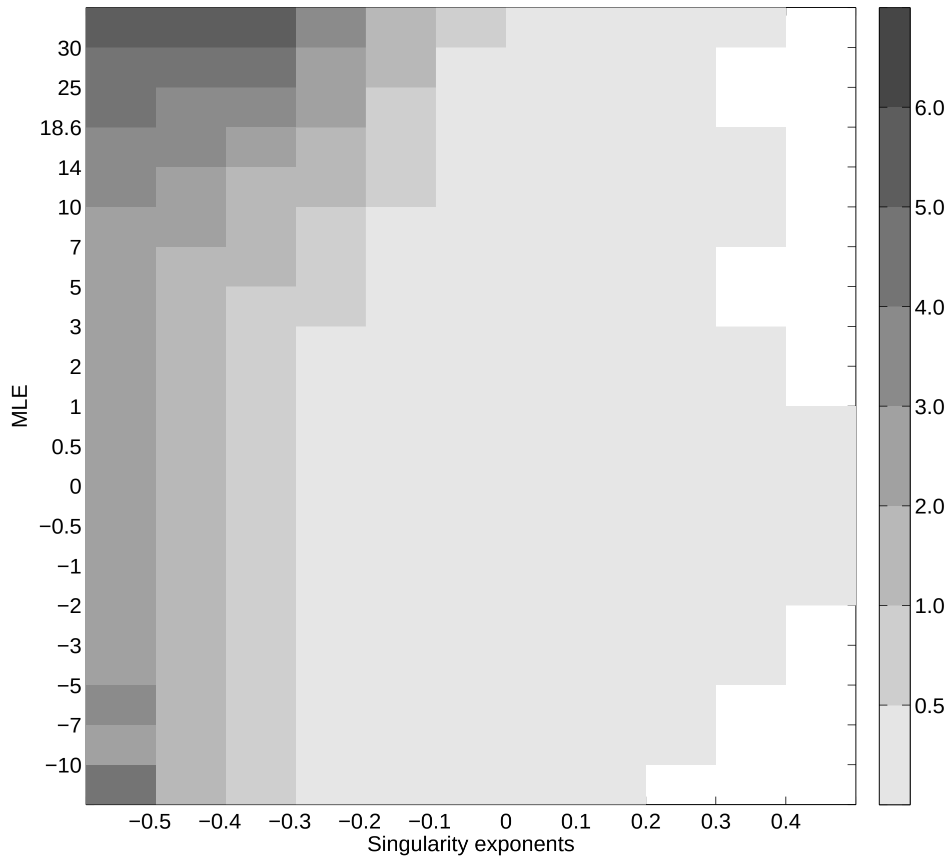


Mean TMI RR as a function SE and MLE. Only the collocations with wind speeds above 4 m/s are used.

# C-band Quality control

- MLE-based QC: WVCs with MLE>+18.6 are filtered
- MLE-/SE-combined QC: WVCs with MLE >+18.6 or SE<-0.45 are filtered
- MUlti-Dimensional Histogram (MUDH): MLE-/SE-combined QC, but analyzed at different wind speed and measurement variability factor ($K_p$) categories.

| V≥4 m/s | VRMS (Rejected WVC) | | | VRMS (Kept WVC) | | | QC-ed ratio (%) | | |
|---|---|---|---|---|---|---|---|---|---|
| | MLE | MLE/SE | MUDH | MLE | MLE/SE | MUDH | MLE | MLE/SE | MUDH |
| 10-min buoy wind | 5.04 | 5.28 | 5.21 | 1.63 | 1.62 | 1.61 | 0.32 | 0.65 | 1.04 |

# An example

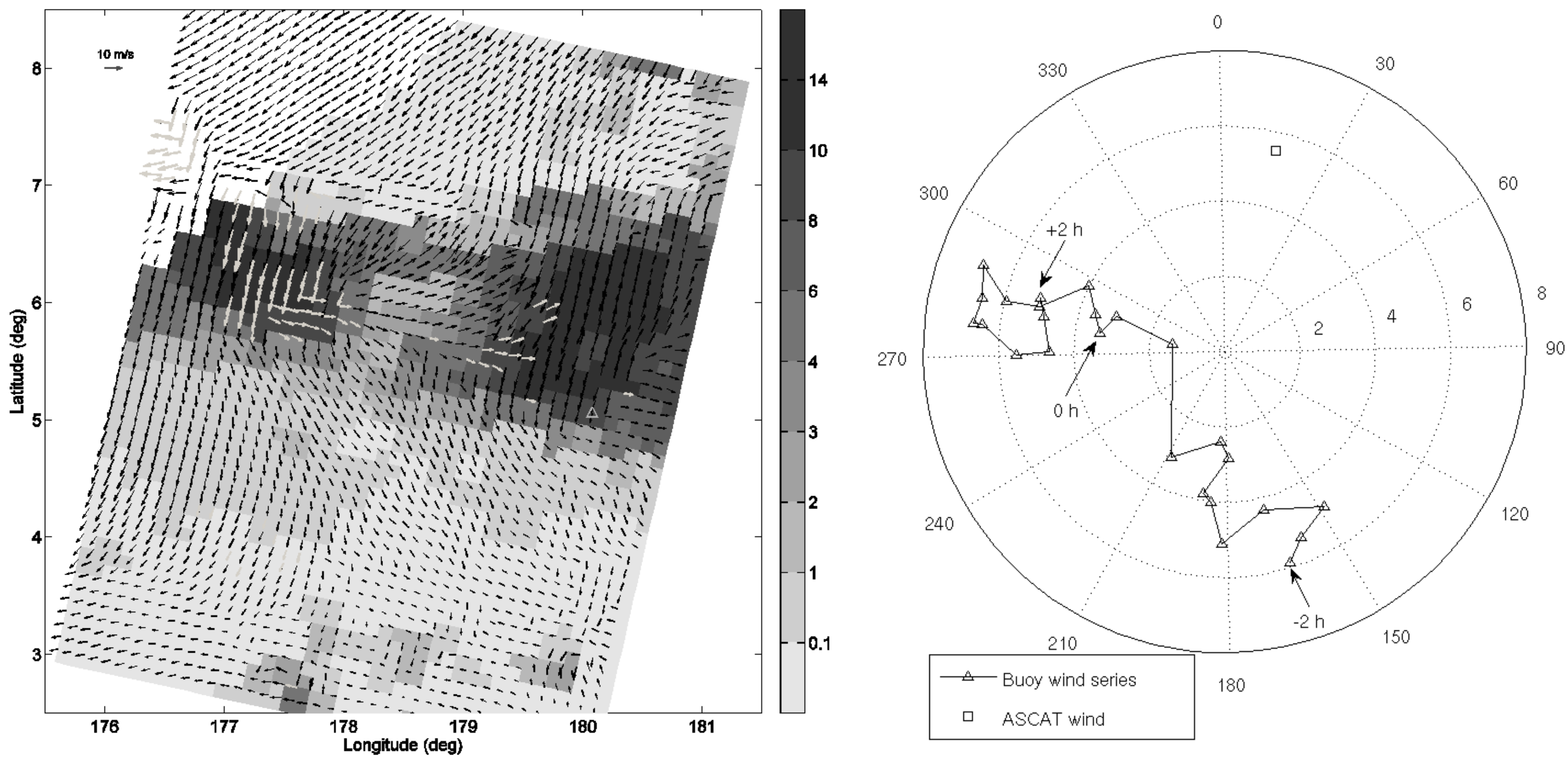


(*a*) (*b*)

Fig.2 (*a*) ASCAT wind observed on December 15, 2009, at 21:17 UTC, with collocated TMI RR superimposed (see the legend). The black arrows correspond to QC-accepted WVCs, and the gray ones correspond to QC-rejected WVCs. The buoy measurements (denoted by the triangle) were acquired at 21:20±2 hours UTC, as shown in the polar coordinate plot (*b*).

# An example

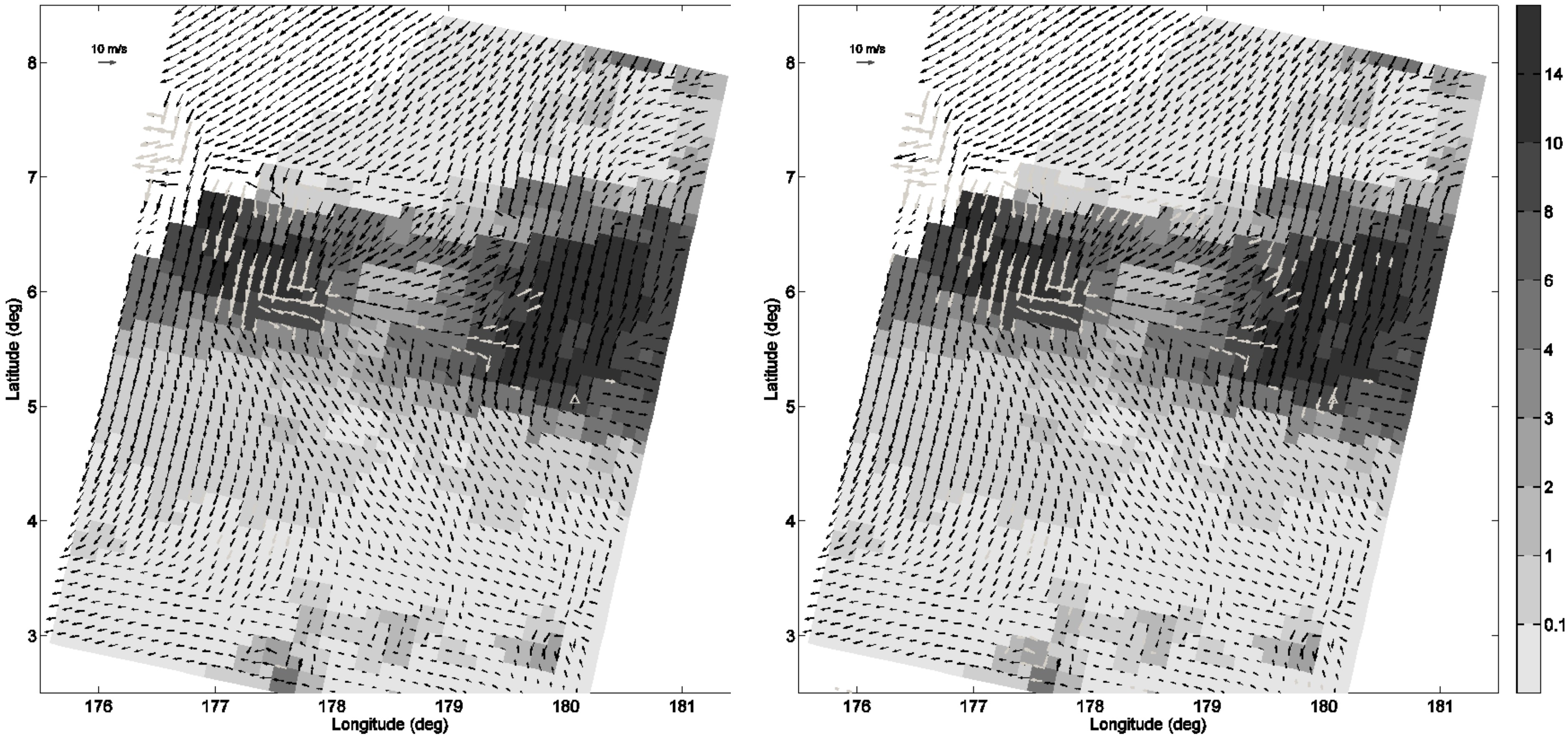


(*c*) (*d*)

Fig.2 Illustration of the rejected WVCs (gray arrows) using (*c*) the combined SE/MLE analysis and (*d*) the MUDH technique. The gray ones correspond to QC-rejected WVCs. The buoy measurements (denoted by the triangle) were acquired at 21:00 UTC.

# An example

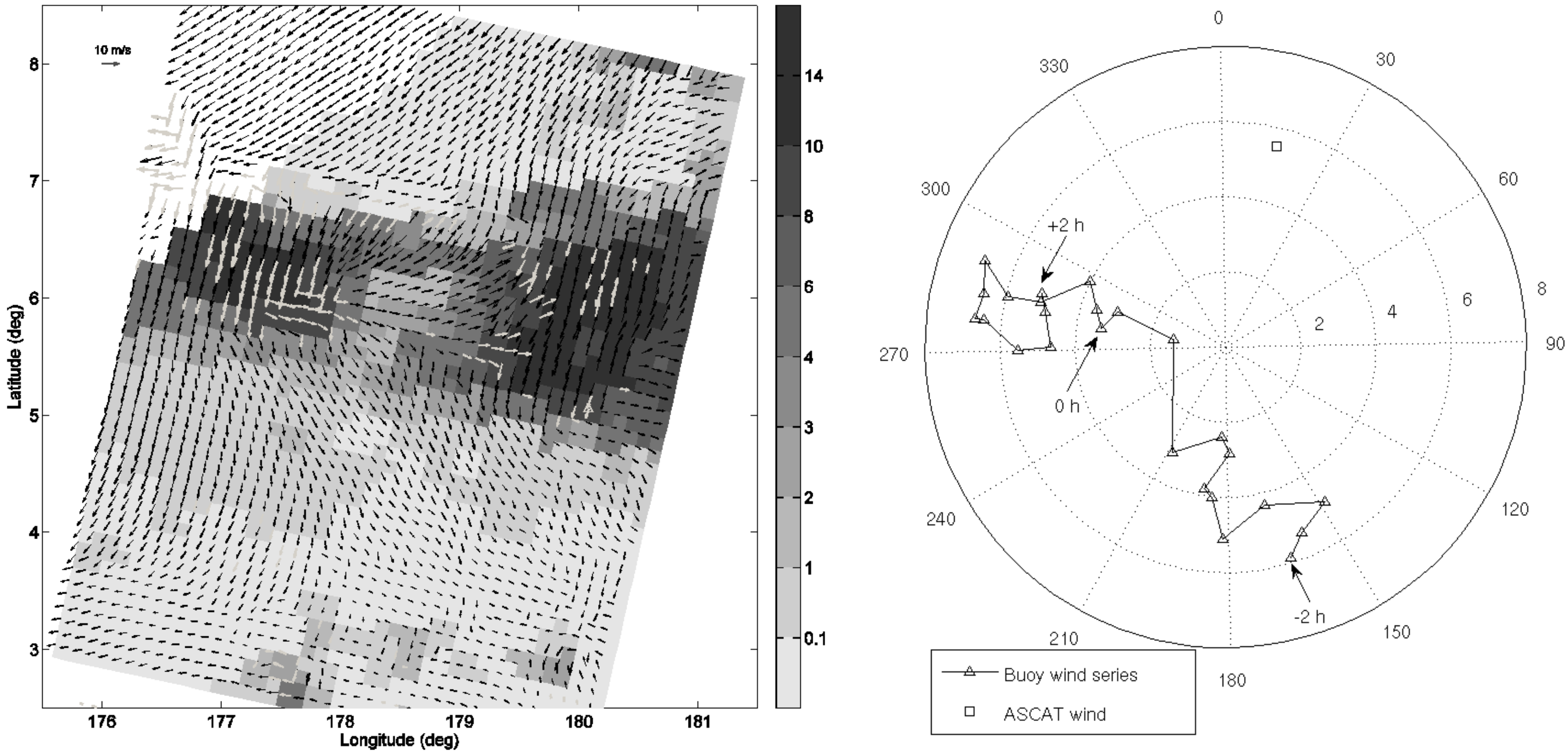


(*a*) (*b*)

Fig.2 (*a*) ASCAT wind observed on December 15, 2009, at 21:17 UTC, with collocated TMI RR superimposed (see the legend). The black arrows correspond to QC-accepted WVCs, and the gray ones correspond to QC-rejected WVCs (MUDH). The buoy measurements (triangles) were acquired at 21:20±2 hours UTC, as shown in the polar coordinate plot (*b*).

# Sub-cell wind variability

| | SD (speed, m/s) | SD (direction, °) | SD (u, m/s) | SD (v, m/s) |
|---|---|---|---|---|
| MLE | 1.24 | 27.7 | 1.66 | 1.62 |
| SE/MLE | 1.27 | 32.1 | 1.62 | 1.61 |
| MUDH | 1.29 | 34.9 | 1.60 | 1.73 |
| \|MLE\|<0.5, SE>0 | 0.37 | 6.3 | 0.47 | 0.52 |

- MLE & SE are indeed good sub-WVC wind variability indicators
- Sub-WVC variability well correlates with buoy verification

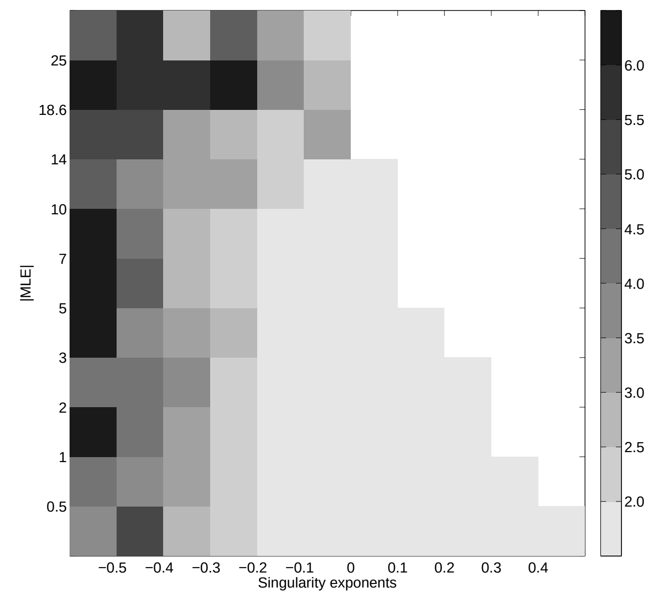

# Quality verification

- Mean buoy winds (25-km-equivalent)

$$\overline{\varphi} = \arctan\left(\frac{-\overline{u}}{-\overline{v}}\right)$$

$$\overline{w} = \frac{1}{M}\sum_{i=1}^{M} w_i$$

where
$$\begin{cases} \overline{u} = \frac{1}{M}\sum_{i=1}^{M} -w_i \sin(\varphi_i) \\ \overline{v} = \frac{1}{M}\sum_{i=1}^{M} -w_i \cos(\varphi_i) \end{cases}$$

| V≥4 m/s | VRMS (Rejected WVC) | | | VRMS (Accepted WVC) | | | QC-ed ratio (%) | | |
|---|---|---|---|---|---|---|---|---|---|
| | MLE | MLE/SE | MUDH | MLE | MLE/SE | MUDH | MLE | MLE/SE | MUDH |
| 10-min buoy wind | 5.04 | 5.28 | 5.21 | 1.63 | 1.62 | 1.61 | 0.32 | 0.65 | 1.04 |
| Mean buoy wind | 4.25 | 4.41 | 4.45 | 1.29 | 1.28 | 1.27 | - | - | - |

- By using mean buoy winds, the variance reduction is about 30-40% in both accepted and rejected categories
- Sub-WVC wind variability is therefore the dominant factor for quality degradation (in both wind sources!)

***Lin et al., TGRS, 2015***
***Lin et al., TGRS, in press***

# Ku-band Quality Control (RapidSCAT)

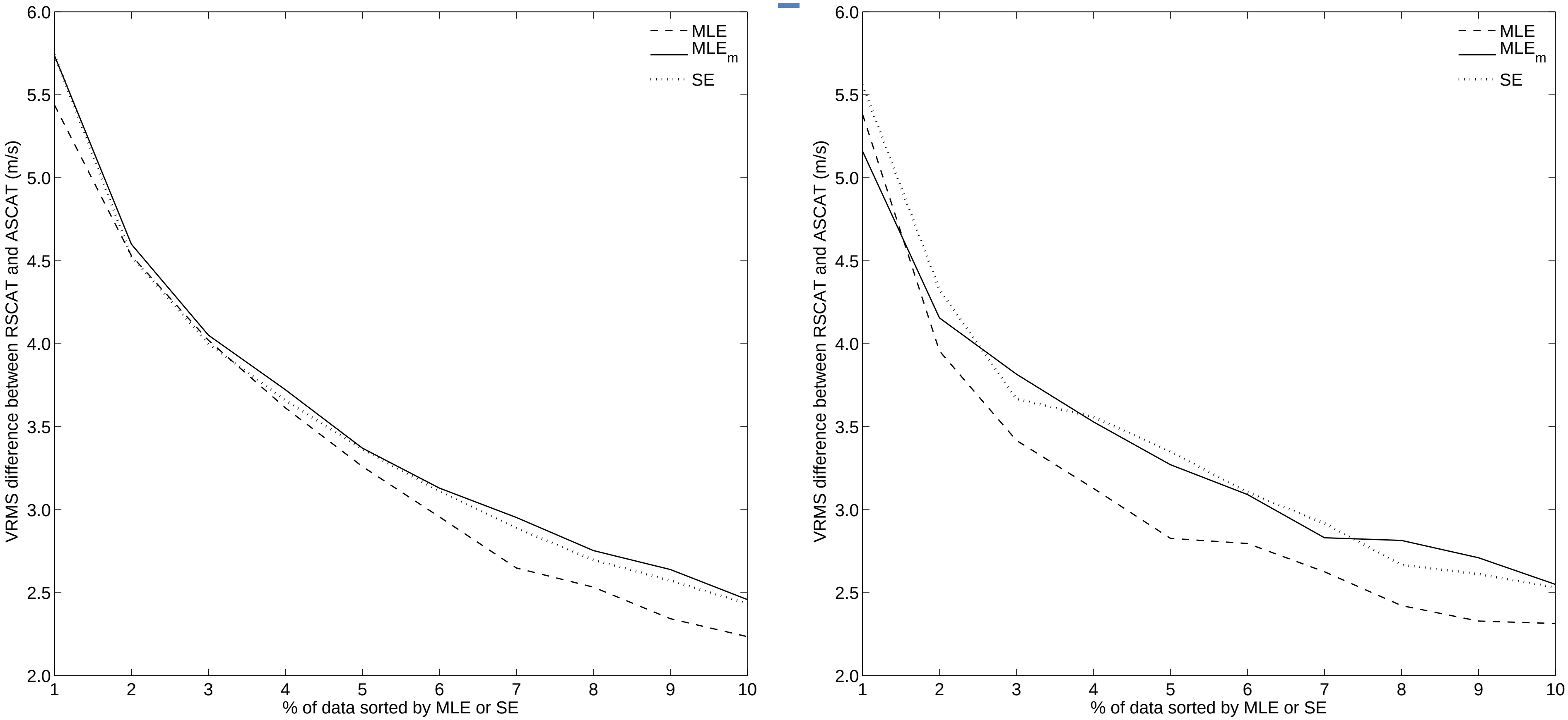


The Vector Root-Mean-Square (**VRMS**) difference between **RSCAT and ASCAT** as a function of the sorted percentiles by MLE or SE (left) Inner swath; (right) Outer swath.

***Lin et al., JSTARS, in preparation***

# Situation-dependent O/B errors

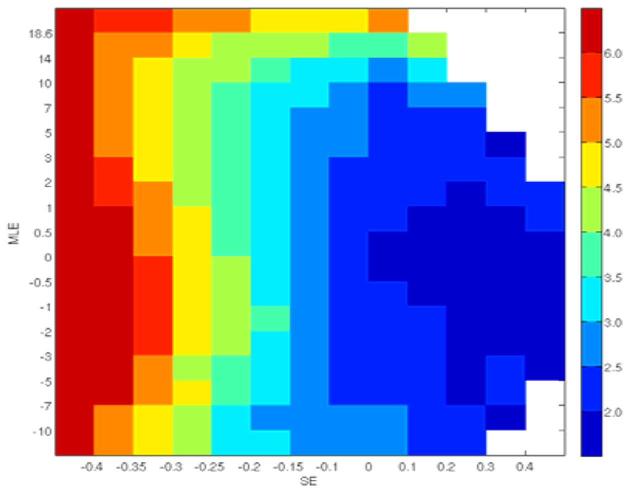


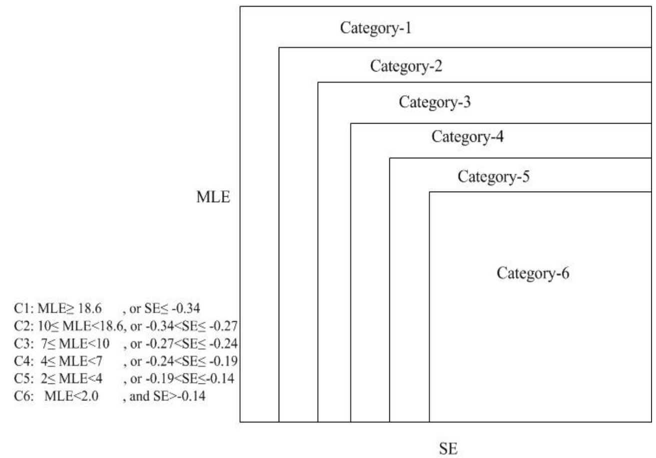


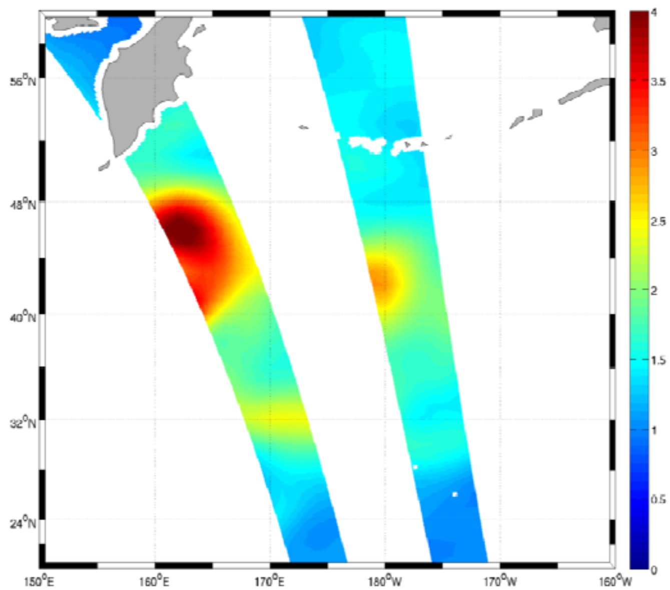


ECMWF Ensemble Data Assimilation
(EDA background error)

***Lin et al., JGR, 2015***

# Results: Typhoon Chan-hom

**ECMWF speed+vector**

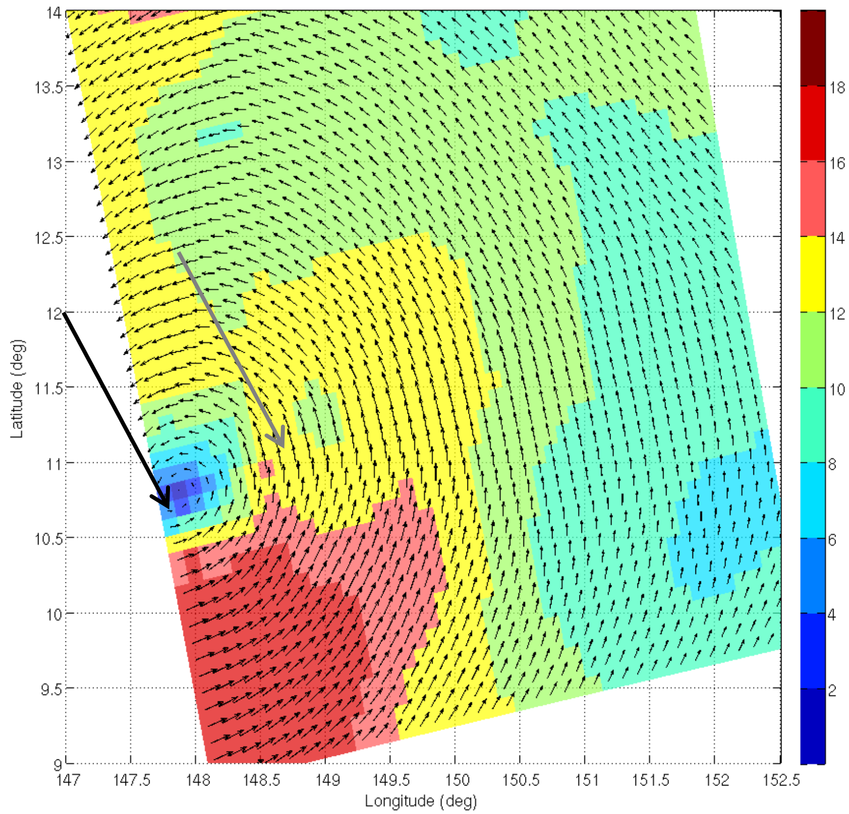


**ASCAT ambiguities**

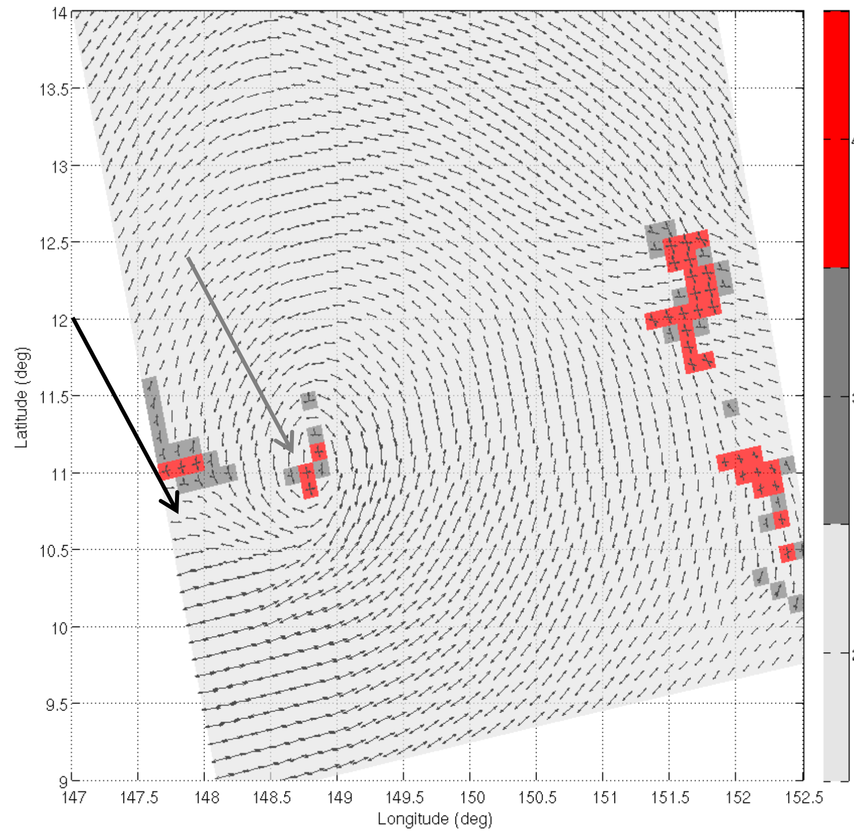


Typhoon Chan-hom (early stage) July 3rd, 2015.

Colorbar: wind speed

Colorbar: number of ambiguities

*Lin et al., Quart. J. R. Met. Soc., in press.*

# Results: Typhoon Chan-hom

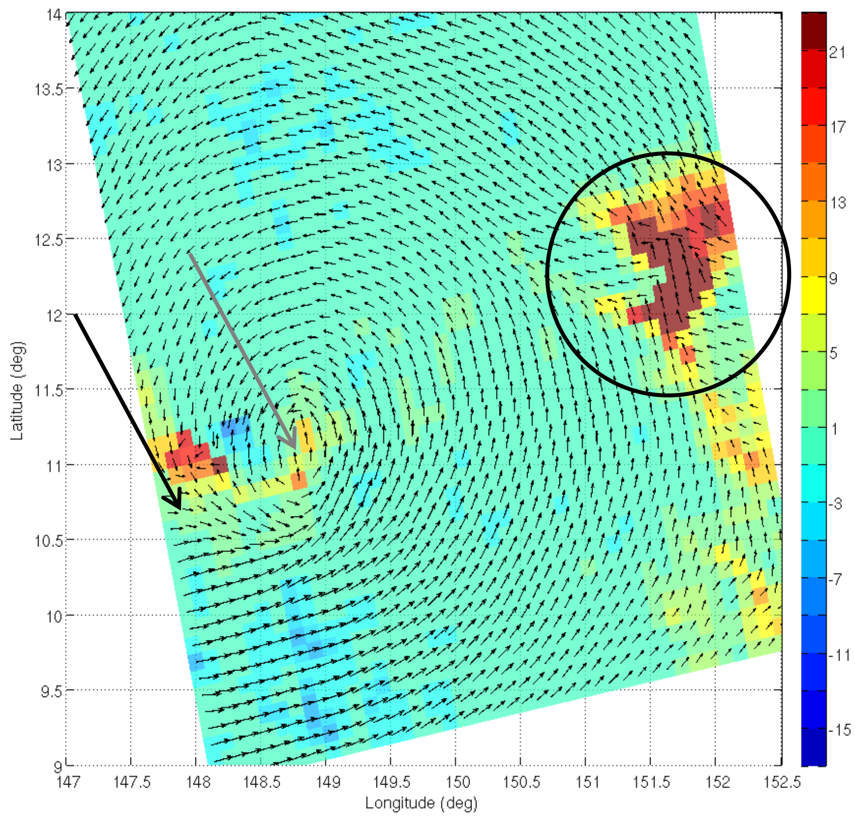


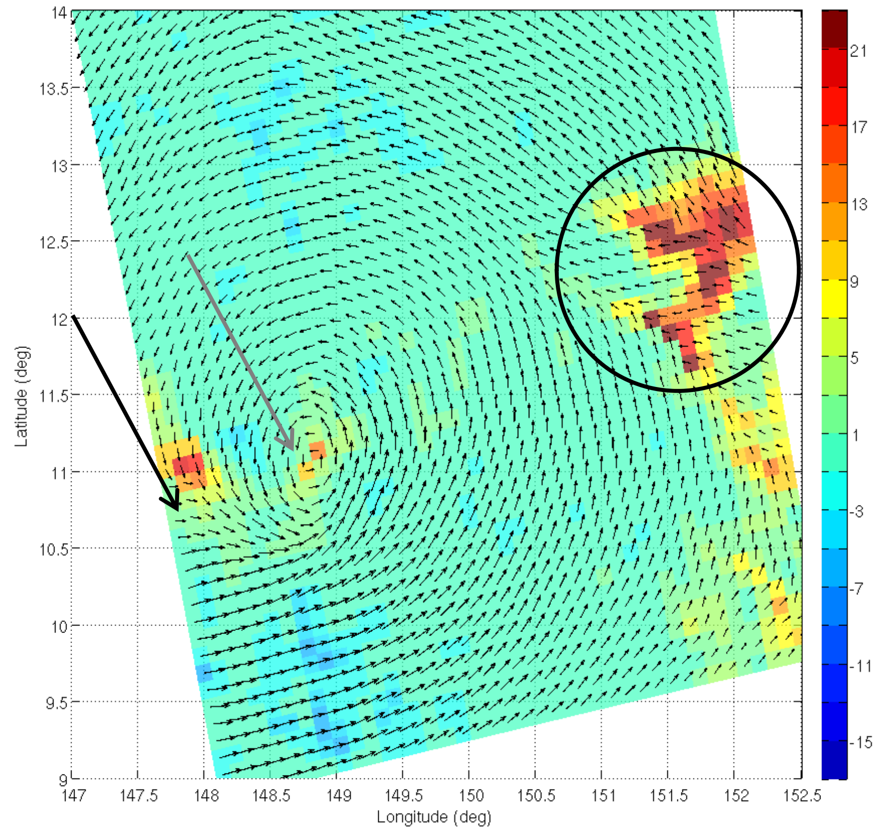


**Default setting:**

- Gaussian structure function
- Fixed O/B errors

**Proposed setting:**

- Numerical structure function
- Flexible O/B errors

ASCAT selected MLE (color)+vector (arrows)

# Rain Effects

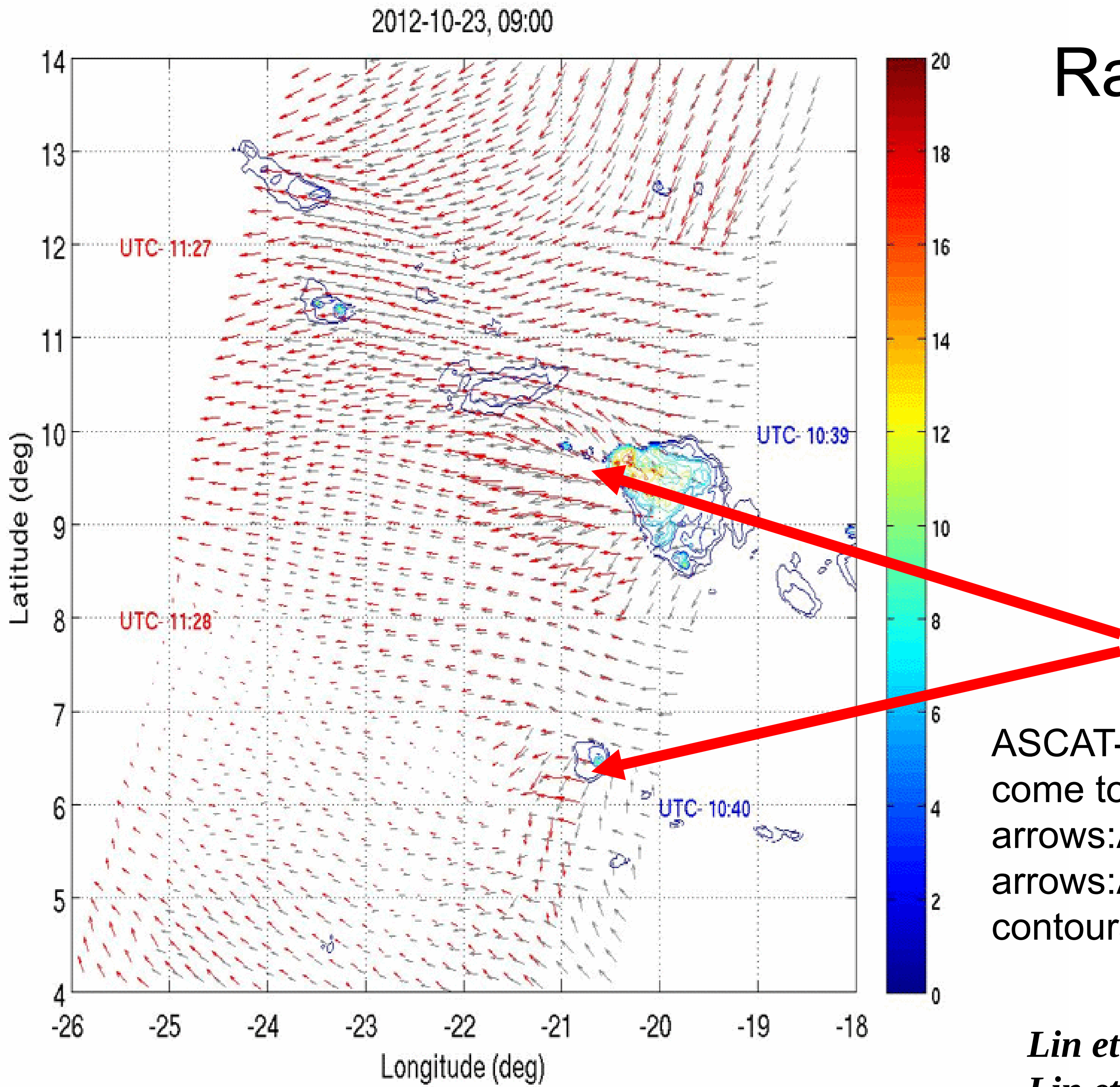


ASCAT-A and ASCAT-B come together. Red arrows:ASCAT-A; Blue arrows:ASCAT-B; color contours: MSG RR.

***Lin et al., GRSL, 2014***
***Lin et al., TGRS, 2015***

ASCAT-B
Nearest-in-time
at k = 7

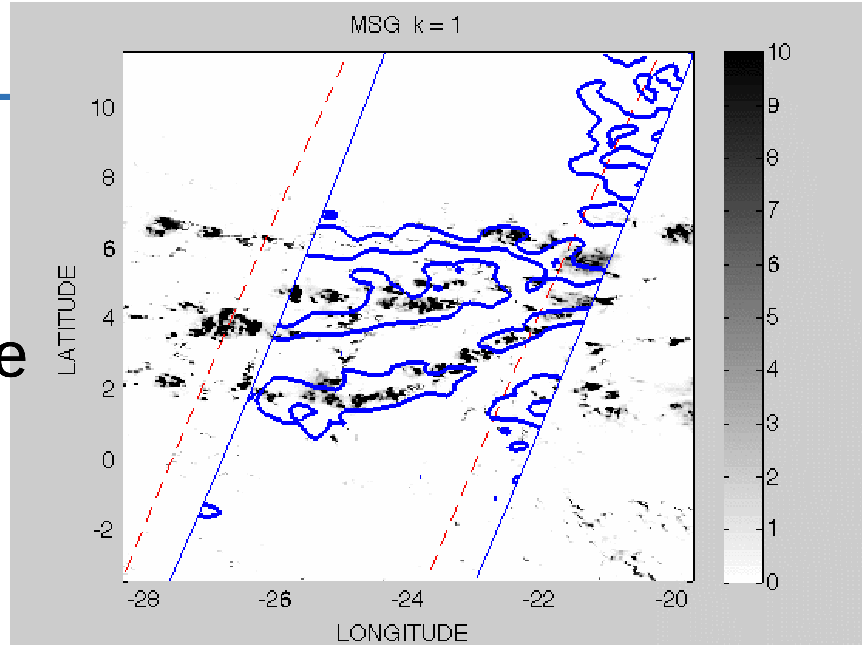


Contours
SE = -0.1

Animation of
17 frames of MSG
(15 minutes apart)

ASCAT-A
Nearest-in-time
at k = 10

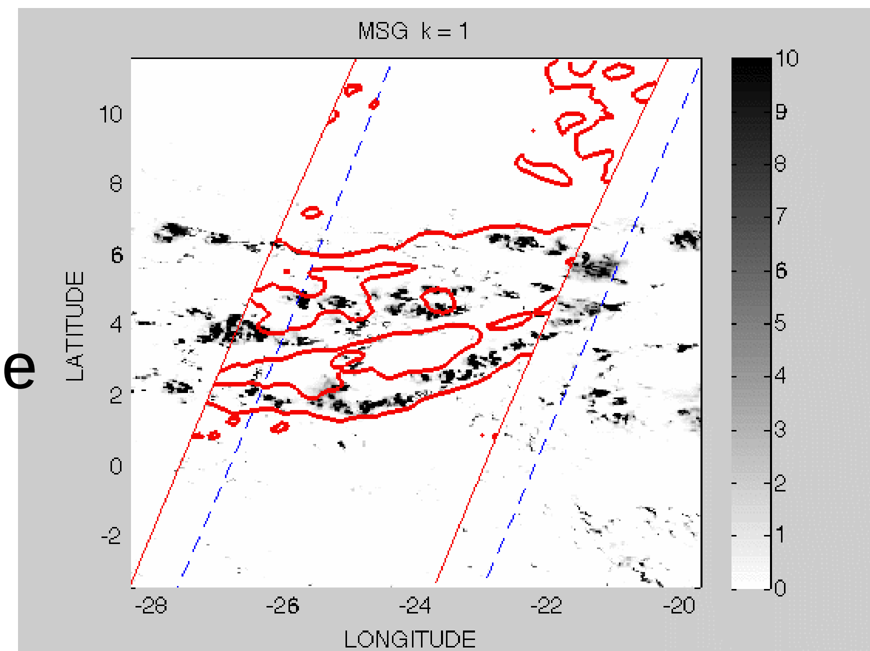

# Conclusions

- Singularity analysis is a powerful image processing tool
- Singularity exponents reveal a common property of the ocean scalars (passive, active, and reactive), i.e., the advection term
- SA is successfully adapted for scatterometer QC
- Both MLE and SE are sensitive to sub-cell wind variability
- SA is currently being applied to scatterometer QC, wind field analysis (e.g., under rain), and ambiguity removal
- SA will soon be applied to scatterometer wind data assimilation